An Exploration of Through-the-Eyelid Tonometry

by

Suzette D. Vandivier

Submitted to the Department of Electrical Engineering and Computer Science

in Partial Fulfillment of the Requirements for the Degree of

Master of Engineering in Electrical Engineering and Computer Science

at the Massachusetts Institute of Technology

May 11, 2001 [June 2001]

Author_____
Department of Electrical Engineering and Computer Science
May 11, 2001

Certified by_____
Stephen K. Burns
Thesis Co-Supervisor

Certified by_____
David Miller
Thesis Co-Supervisor

Accepted by_____
Arthur C. Smith
Chairman, Department Committee on Graduate Theses

An Exploration of Through-the-Eyelid Tonometry
by
Suzette D. Vandivier

Submitted to the
Department of Electrical Engineering and Computer Science

May 11, 2001

In Partial Fulfillment of the Requirements for the Degree of
Master of Engineering in Electrical Engineering and Computer Science

Abstract

The use of through-the-eyelid tonometry to determine the intraocular pressure (IOP) of the eye for glaucoma screening may improve patient comfort by deforming the cornea through a closed eyelid rather than directly. Two techniques to determine IOP are proposed and evaluated. The first method requires a determination of the beginning point of corneal applanation from a force-indentation curve of the eyelid and cornea in series. Eyelid and cornea frequency dependence data as well as force-indentation curves were obtained on one subject in a supine position. Measurements indicate differing stiffness ranges for the eyelid and cornea, however, the force-indentation curves only slightly suggest these differences. The second tonometry method requires a 3d plot of eyelid/cornea ultrasound scans versus increasing applied force to recognize decreasing corneal echo width as the eyelid and cornea are flattened. 3d plots were obtained from indenting 3 pliant hemispheres with an ultrasound probe. The expected echo width trends during surface applanation were unrecognizable. Further exploration is needed to determine the viability of both proposed tonometry techniques.

Thesis co-supervisor: Stephen K. Burns
Title: Senior Research Scientist, HST

Thesis co-supervisor: David Miller
Title: Associate Clinical Professor of Ophthalmology, Harvard Medical School

Table of Contents

Acknowledgements

I would like to thank the following people:

Dr. Stephen Burns for his many ideas, good advice, and especially for constructing the ultrasound system probe.

Dr. David Miller for his helpful feedback, wealth of ophthalmology knowledge, and contact suggestions.

Ryan Carlino for his near instantaneous email responses to numerous software and hardware questions.

Mark Ottensmeyer for allowing me to use his device, aiding me in take several hours of data, and for being willing to continue helping with the project after I leave.

The librarians at the New England College of Optometry for always being willing to track down a long lost article even if it is in German and has been out of print for ages.

To R. Erich Caulfield for always letting me bounce ideas off him even when I made no sense.

To R. John Thomas for insisting (thank heavens) on doing one last edit session, even though I was ready to go to the printers.

To Yamel Cuevas, Erik Island, Shawn Kelly, and Anand Patel for letting me "poke" their eyes.

To my mother for responding to countless "I'll never finish" phone calls with "Then just drop out".

Chapter 1

Introduction

Glaucoma is a damaging condition of the eye typically characterized by an abnormally high intraocular pressure (IOP) which can cause vision impairment ranging from temporary effects to permanent blindness. Several different eye diseases can cause glaucoma making it the third most common eye affliction affecting over 65 million people world wide[9]. Early detection and risk assessment are key to early treatment which may minimize the risks or the effects of glaucoma.

The tonometer is an important diagnostic device which determines the IOP of the eye by measuring the force necessary to apply a specific deformation to the cornea. Several relatively non-invasive tonometers exist including applanation, indentation, and non-contact air jet tonometers. All routine eye check-ups involve a tonometer reading to screen for glaucoma.

The non-contact air jet tonometers are the most commonly used devices in optometrists' offices today because they are the least invasive and require the least skill to operate. However, they are not as accurate as contact tonometers and are used only as an initial glaucoma screening device[13]. Direct contact to the cornea can be an uncomfortable and unnerving procedure. A less invasive yet still accurate tonometry technique would be more appealing and could lead to fewer inaccuracies due to patient nervousness. One possible technique is to apply the deformation required for IOP measurement through the closed eyelid to the cornea.

1.1 Anatomy and Mechanics

Before exploring novel through-the-eyelid tonometry techniques, a careful study of the anatomy and mechanical properties of the cornea and eyelid as well as current tonometry techniques is needed.

1.1.1 Cornea

The anatomical and mechanical characteristics of the cornea are essential to relating corneal deformations to the intraocular pressure of the eye. The eye is essentially spherical except where the cornea bulges outward as shown in Figure 1.0.

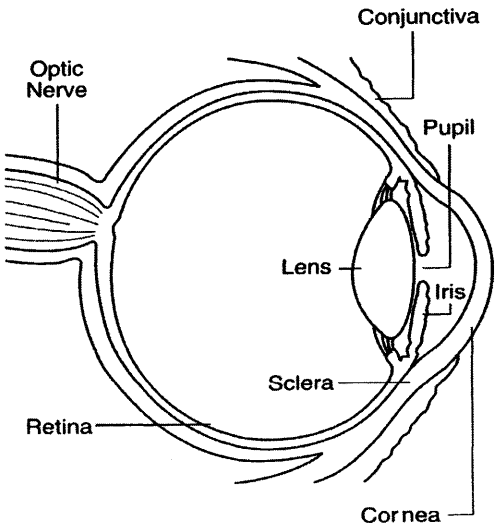

Figure 1.0: Eye anatomy.

The cornea is spherical within approximately 1.5mm of the center with a curvature in the range 5.5mm to 9.5mm [16], an average central thickness of 0.55mm [21], and an average ocular rigidity* of 0.0245 V^{-1} [16]. Although the compressibility of the eye is not often presented in force per unit length as with many tissues, the compressibility of the eye can be approximated to 100N/m[22]. The radius of curvature of the center of the cornea can be non-invasively measured using a standard Keratonometer. Many factors affect the dimensions and mechanical properties of the cornea including age, gender, and race[16]. Corneal variations require tonometry techniques with limited dependence on specific corneal characteristics.

* Ocular rigidity is a measure of the distensibility of the eye which relates applied pressure to deformation volume. See Section 1.2.1.

1.1.2 Eyelid

The eyelid shown in Figure 1.1 has four layers: the skin, a striated muscle layer, a fibrous tissue layer, and the conjunctiva[17] (the thin mucus membrane on the underside of the eyelid). The part of the eyelid which covers the eye is relatively uniform in layers and has an average thickness of 2mm [17].

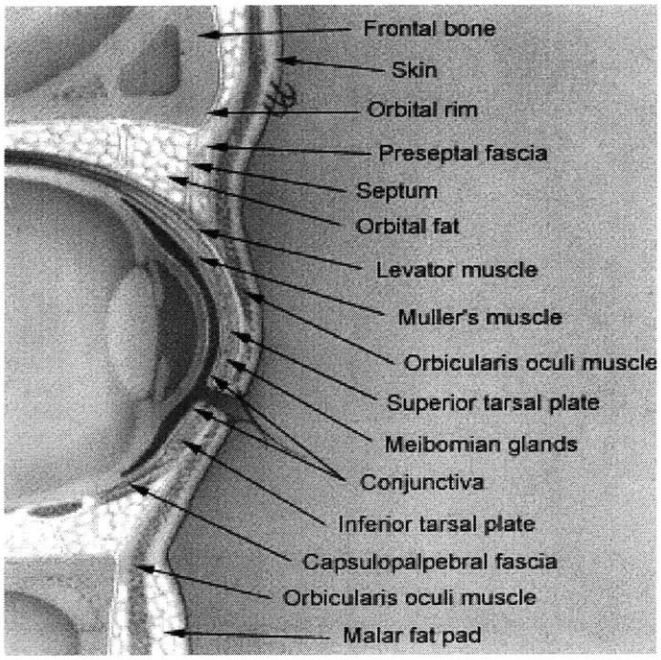

Figure 1.1: Eyelid Anatomy[17]

Little research has been conducted on the specific mechanical properties of the eyelid, and simple modelling of the eyelid based on soft tissue or skin modelling is complicated by the eyelid's layered anatomy. Mechanical trends in facial skin and tissue, however, have been well researched and may be exhibited by the eyelid as well. Pierard et al. observed a significant increase in facial skin extensibility and a significant decrease in elasticity with ageing in women[15]. Takema et al. reported an increase in the elasticity coefficient of the facial skin, as well as an increase in the thickness of the skin of the forehead, corners of the eyes and cheeks with age[19]. Reported stiffness measures range greatly due to a strong dependence on tissue thickness and experimental methods, thus exact stiffness values are not useful for comparison with corneal stiffness values. However, the reported facial tissue trends do suggest that the thickness and mechanical properties of the eyelid could be affected by age. Eyelid variability requires the development of through-the-eyelid tonometry techniques which minimize dependence on eyelid characteristics.

1.1.3 Soft Tissue

Even though the mechanical properties of the eyelid have not been researched, it is useful to look at generic tissue stress-strain models. Mathematical relations used to model soft tissue are determined by matching potential models to experimental data. Fung[11] outlines several basic soft tissue models including the Maxwell Model, the Voigt Model, and the three-element Kelvin model (a standard linear solid), depicted in Figure 1.2. These models consist of springs and dashpots in various configurations.

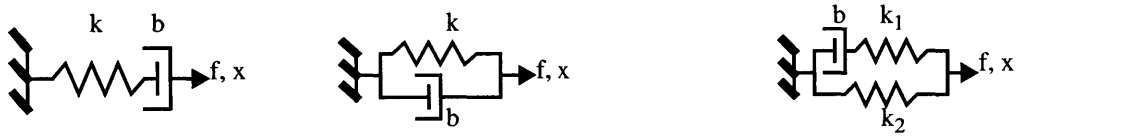

$$x = \left(\frac{1}{k} + \frac{1}{b}\int dt\right) f \qquad f = \left(k + b\frac{d}{dt}\right) x \qquad \left(\frac{b}{k_1}\frac{d}{dt} + 1\right) f = k_2\left(b\frac{(k_1 + k_2)}{k_1 k_2}\frac{d}{dt} + 1\right) x$$

(a) (b) (c)

Figure 1.2: Maxwell (a), Voigt (b) and Kelvin (c) bodies.

Most biological tissues are considered viscoelastic, and thus exhibit three specific tissue behaviors: creep, stress relaxation, and hysteresis. Creep is the phenomena in which an applied constant stress to a body results in a continued deformation of the body. Stress relaxation is the phenomena in which a body undergoes a constant strain and the resulting stress on the body decreases with time. Hysteresis is the phenomenon in which a material reacts differently in a cyclic loading process than in a cyclic unloading process. As shown in Figure 1.3, each of the three models captures only part of the behavior of soft tissues.

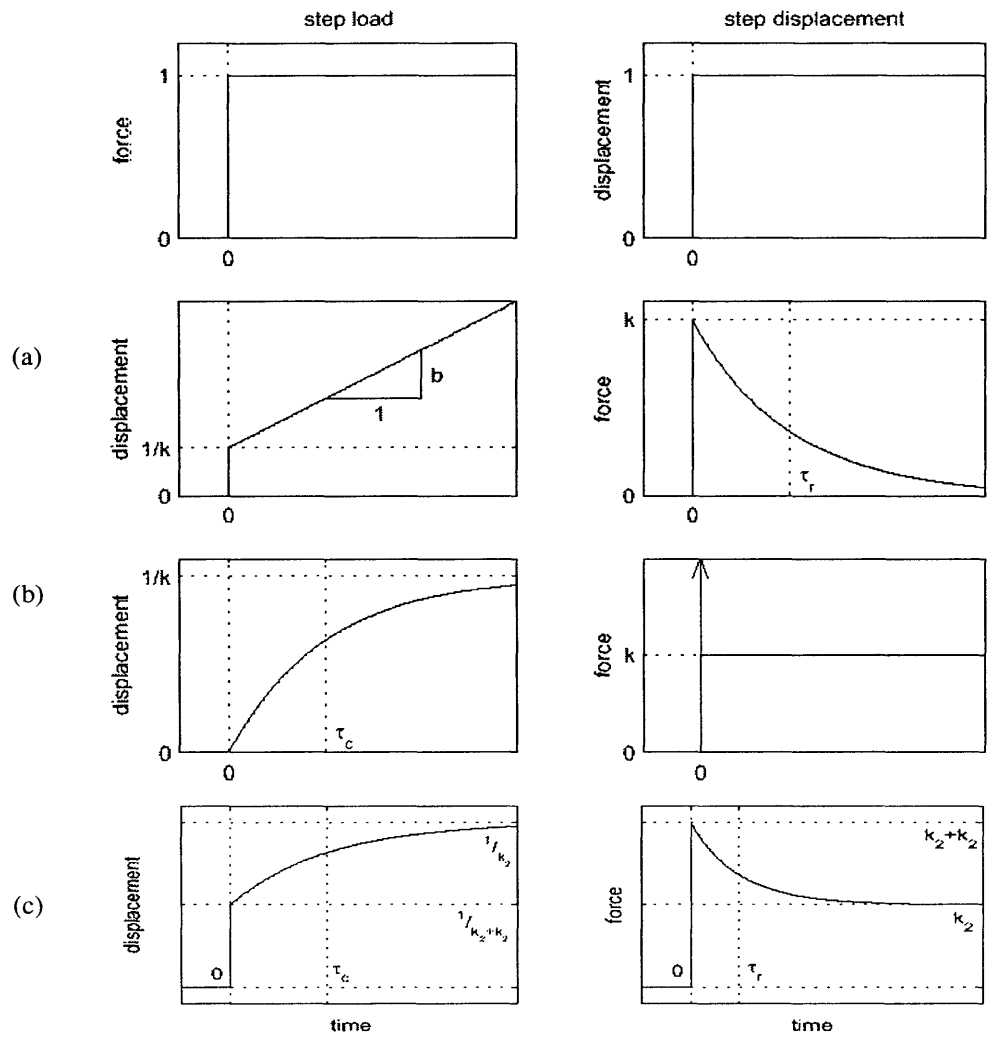

Figure 1.3: Creep and Stress Relaxation characteristics of a Maxwell (a), Voigt (b) and Kelvin (c) body.[14]

Most biological tissues exhibit continuous creep under a step force to a final length. This behavior is captured by the Voigt and Kevin bodies, but not the Maxwell body. The Voigt body exhibits an impulse response in force to a step in deformation, which is not an observed tissue behavior. An initial elastic response to step loads observed in most biological tissues is also exhibited by the Kelvin and Maxwell bodies.

Because viscoelastic materials exhibit hysteresis, a simple finite deformation experiment would not result in a valid stress-strain relation. Instead, it is necessary to apply a periodic oscillatory deformation. After several loading and unloading cycles, the tissue is considered preconditioned. In essence, the tissue is transformed into a tissue with repeatable, consistent mechanical properties. Experimental data taken after preconditioning is predictable and, thus, can be used to match a model.

1.2 Tonometry

Tonometers are clinical devices used to determine the intraocular pressure of the eye. There are two main contact tonometry techniques, indentation and applanation tonometry. Both involve minimally deforming the cornea and using a force-indentation relation to determine the intraocular pressure from the deformation and applied force.

1.2.1 Indentation Tonometry

Indentation tonometry involves applying a specific weight to the cornea and measuring the resulting indentation depth. The Schiotz tonometer is the most common indentation tonometer and consists of a freely sliding plunger enclosed by a shaft which is attached to a concave footplate as depicted in Figure 1.4.

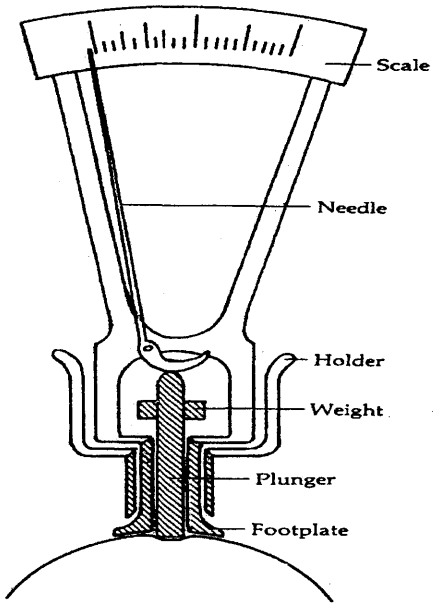

Figure 1.4: Shiotz Tonometer[16]

A weight is attached to the plunger, and the device is placed on the anesthetized cornea with the patient lying face up. The indentation distance, D, and plunger weight, W, are converted to the measured intraocular pressure, P, by the Shiotz relation.

Shiotz's formula can be derived by starting with Fick's law[7] for spheres

$$P = \frac{W}{A}$$

and calculating the area of the indentation. The radius of the indented region R is assumed to be linearly dependent on the indentation D such that

$$R = a + bD$$

where a and b are constants. Thus the area of the indentation is

$$A = \pi R^2 = \pi(a + bD)^2$$

and the final stress/strain relation is

$$P = \frac{W}{\pi(a + bD)2}$$

While investigating the accuracy and required calibration of indentation tonometers, Friedenwald determined that for D less than 4.82mm, P was related to D by following relation[7,7].

$$P = \frac{W}{a + bD}$$

These two relations continue to be accepted today for indentation tonometry, and the only discrepancy in experimental study lies in the choice of the constants a and b. Friendenwald matched the relations to experimental data using the following constants.

$$P = \frac{W}{7.75 + D} \quad \text{for D<4.82}$$

$$P = \frac{W}{(2.92 + 0.13)2} \quad \text{for D>4.82}$$

The deformation caused by the tonometer results in a measured IOP that is not equivalent to the actual IOP since corneal indentation causes the IOP to change slightly. Thus, a formula relating the measured pressure (P) and the actual pressure (P_o) is needed. Friedenwald developed a pressure-volume relation which can be used to determine P_o from P. He determined that a change in volume of the eye relates to the intraocular pressure by

$$\Delta V = \frac{\left(\log\left(\frac{P}{P_o}\right)\right)}{K}$$

where K is defined as ocular rigidity, a measure of distensibility of the cornea, with units of inverse volume. If the pressures due to two different weights are measured and the volume changes due to the indentations are calculated, then K and P_o can be determined. The volume of the eye deformed by a particular indentation depth can be calculated by realizing that the indentation shape is approximately that of a truncated cone. Thus, the volume of indentation can be calculated from

$$V = \frac{\pi}{3}[(a + bD)^3 - a^3]$$

One incorrect assumption in Friedenwald's equation is that K is constant for a particular eye regardless of imposed deformation[10]. Instead, K actually decreases as the IOP due to the tonometer deformation increases[22]. However, Friedenwald established that the effective change in K due to the indentation is essentially negligible. Other volume/pressure relations have been proposed since Friendenwald's initial formulation[7,15,23]. Greene provides a detailed comparison of these relations[10].

1.2.2 Applanation Tonometry

Applanation tonometry involves applying a force to the eye sufficient to flatten the cornea a specific area A_i. Goldmann tonometry involves the patient sitting up, face straight forward, and the addition of a small amount of fluorescein and a drop of anesthetic to the tear film. The tonometer is mounted level and hinged on a slit-lamp. As shown in Figure 1.5, a biprism applanator creates two semicircles when it contacts the treated cornea. The force applied by the biprism is increased until the inner margins of the semicircles touch, indicating that the applanated region equals 3.06mm in diameter. This diameter was chosen in order to simplify pressure conversions.

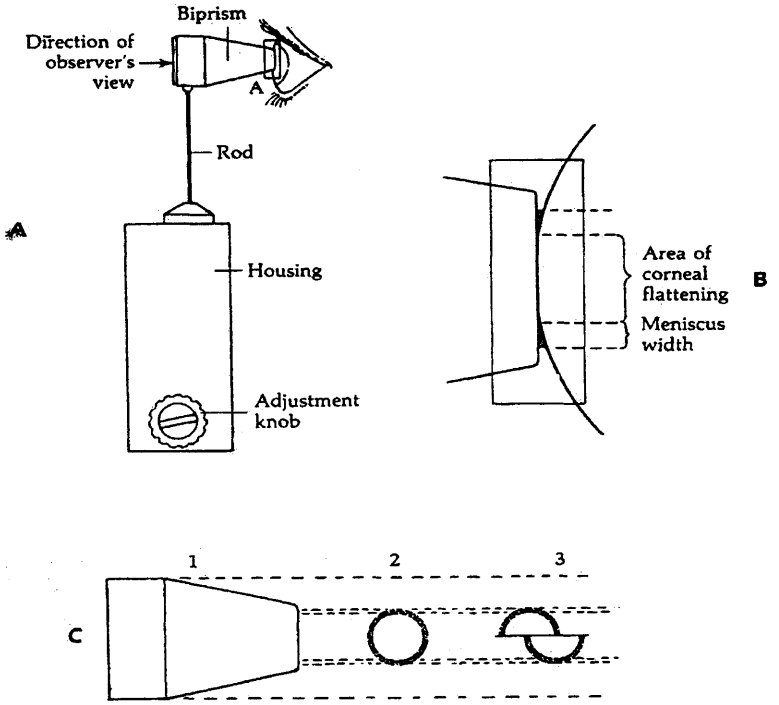

Figure 1.5: A) Goldmann Tonometer B) Corneal Applanation C) Semicircles create by biprism applanator[16].

The force required to flatten a spherical, dry, flexible, elastic, and infinitely thin surface is related to the IOP by the Imbert-Fick law

$$P = \frac{F}{A}$$

Since the cornea does not completely fit these requirements, Goldmann made adjustments to this formula. The normal force (N) applied by the cornea to the applanation device in response to the device's force must be added to the pressure, and the surface tension force (M) created between the applanation surface and the tear film which covers the cornea must be added to the force. The pressure/force relation becomes

$$P = \frac{F}{A} + M - N$$

A distinction must be made between the external area of the cornea which is in direct contact with the applanation surface and the internal area. The area in the above equation is the internal flattened area of the cornea. Goldmann and Schmidt set the standard for this area as $7.35mm^2$ and the diameter of the applanation surface as 3.06mm [16]. At this area of flattening, the surface tension force and the normal force are both 0.415 g and cancel each other out [16,21]. Thus, the final relation is

$$P = \frac{F}{7.35mm^2}$$

The imposed deformation due to applanation is small enough that the difference between the measured and actual IOP is considered negligible.

Applanation tonometry is considered the standard rather than indentation tonometry for two main reasons: it imposes a smaller deformation to the eye[16], and it reduces errors due to varying mechanical properties of the cornea[17], i.e. the constancy of K during deformation and the specific curvature of the eye. The Goldmann tonometer does not measure the IOP exactly though. Whitacre et. al. reported that numerous factors introduce error into the IOP measurement including: the exact surface tension of the precorneal tear film, the area and angle of tonometer/tear film contact, ocular rigidity, corneal thickness, the concentration and amount of fluorescein used, the shape of the anterior cornea, and the duration and repeated contact of the tonometer with the eye[21].

1.2.3 Through-the-Eyelid Tonometry

Through-the-eyelid tonometry is a relatively new tonometry technique. Three through-the-eyelid tonometers have been patented in the last decade. In 1993 Fedorov, et al. developed a tonometer involving a free-falling ball dropping on an eyelid-covered cornea[3,4]. The height of the bounce of the ball off the closed eye is then related to the IOP of the eye. In 1994 Suzuki introduced a spring-loaded tonometer with a probe that slides into the eyelid-covered cornea while pressure is being measured[18]. In 1998 Fresco patented a tonometer that involves indenting the cornea through the eyelid until a pressure phosphene is observed by the patient[5,6]. The displacement and applied pressure measured once the phosphene is seen are used to determine the IOP. All three methods require calibration to determine the actual IOP from the measured IOP. None of the techniques detail how the eyelid affects the measured IOP nor how calibration is accomplished. Even though these devices have been patented, no publications seem available describing their use, suggesting that conclusive and validating results are lacking.

Burns and Miller[1] propose two novel through-the-eyelid tonometry techniques. The first involves indenting the cornea through the eyelid with a small diameter probe and measuring relative probe position and corresponding measured force. They speculate that the difference in distensibility of the eyelid and cornea will result in a discontinuity in a force-indentation plot corresponding to the beginning point of corneal applanation. The second technique involves indenting the cornea with an ultrasound probe attached to a force transducer. Ultrasound is often used to determine distances between tissue interfaces. They speculate that a trained technician will be able to extract the necessary information from a 3d plot of the ultrasound scan versus time and measured force to determine the beginning point of corneal applanation and the point at which the cornea has been applanated the complete area of the indenting probe.

1.3 Ultrasound

The basic principle of ultrasound imaging centers on the partial reflections of the initial pulse due to impedance discontinuities in the tissue. Each discontinuity results in an echo. The time between the initial ultrasound pulse and the recorded echos can be used to determine distances between interfaces in an object. If an ultrasound pulse hits a curved surface (or interface), an echo from the center most location on the surface will bounce back first followed closely by echos from the areas just outside the center of the curved surface. The more curved the interface, the wider the overall surface echo.

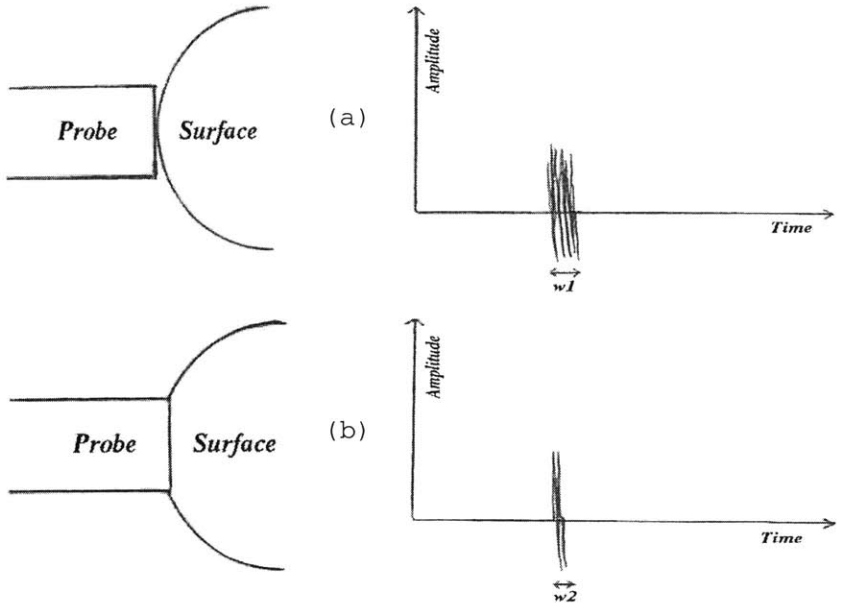

Figure 1.6: a) Ultrasound echo of curved surface. b) Ultrasound echo of flattened surface.

Figure 1.6a shows an ultrasound probe just making contact with a curved surface and an example of what the surface echo might look like. As the probe flattens the surface, the surface echo should decrease in width. Once the surface is completely applanated the area of the probe, the surface echo should be narrow like the one shown in Figure 1.6b.

Chapter 2

Theoretical Methods

In order to explore the viability of the through-the-eyelid tonometry techniques proposed by Miller and Burns, two theoretical methods must be developed. The first method is a mathematical approach to determining the IOP from a model of the force-indentation curve of the eyelid and cornea in series, and the second method is a visual method for determining the beginning and ending points of corneal applanation from a 3d plot of an ultrasound indentation probe where the ultrasound scans are plotted versus measured force. Both methods require the derivation of a pressure equation that will determine the IOP of the eye from the measured forces just prior to corneal indentation and at the exact point of complete corneal applanation with respect to the area of the indenting probe.

2.1 Pressure Equation

As figure 2.0 shows, the cornea and eyelid are idealized as two concentric, spherically symmetric shells. The applanation surface is circular with area A_a and applies a perpendicular force to the shells directly above the cornea. It is assumed that the applanation surface will first flatten the eyelid shell until the inner area is A_e without affecting the inner corneal shell; then the tonometer will apply more force through the eyelid with the flattened internal area of A_e to the cornea until the inner flattened area of the cornea is A_c. It is assumed that the internal area of the eyelid (A_e) is not altered by the additional force needed to flatten the cornea. The areas should fulfill the inequality $A_a >= A_e >= A_c$.

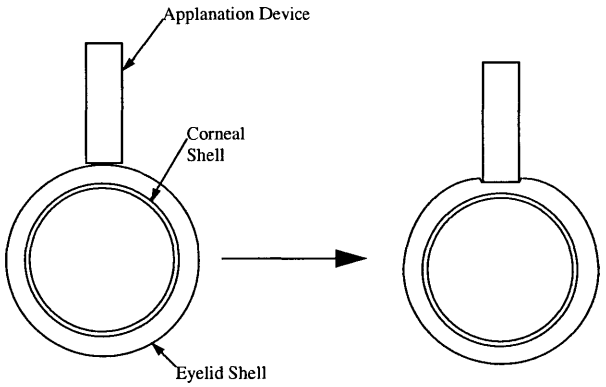

Figure 2.0: Model of cornea and eyelid.

The force (F_e) required to flatten the internal area of the eyelid Ae is related to the normal force (N_e) the eyelid exerts back onto the applanation surface by

$$N_e = \frac{(F_e)}{A_a}$$

The force (F_c) required to flatten the internal area of the cornea Ac is related to the IOP (P) by

$$P = \frac{(F_c)}{A_c} - N_c$$

where N_c is the normal force the cornea exerts back onto the eyelid and F_c is the total force applied by the applanation surface (F_t) minus F_e.

The surface tension force (M) associated with the tear film is ignored in this case since the applanation surface does not contact the precorneal tear film. The eyelid does contact the tear film; however, this contact is initiated before the applanation is performed when the eyelid is closed over the eye. It is assumed that M is incorporated into Ne such that Ne is the true normal force exerted by the eyelid back on to the tonometer minus M.

In order to replicate the measurements of Goldmann type tonometers, Ac should equal $7.35mm^2$ and N_c should equal 0.415g. Only F_t and F_e are necessary to calculate the intraocular pressure of the eye.

$$P = \frac{(F_t - F_e)}{7.35mm^2} - 0.415g$$

2.2 Force-Indentation Method

One method for determining F_t and F_e, requires a plot of applied force versus the deformation depth of the eye and eyelid in series. Figure 2.1 shows a characteristic plot of deformation versus applied force.

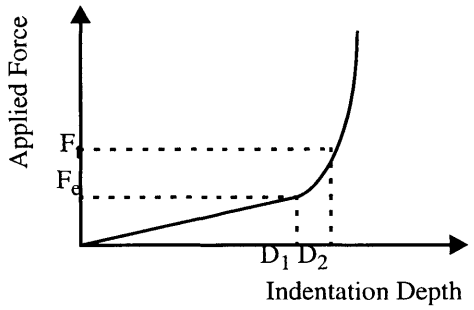

Figure 2.1: Force-Indentation Curve of Eyelid and Cornea

In order to determine an accurate force indentation model of the eyelid, extensive experimental data including eyelid mechanical variability data would be needed. An estimation can be made without experimental data by recognizing that the relative rate of deformation of the eyelid when compared to that of the cornea is essential to determining the point at which the cornea begins to flatten. Since the eyelid is a soft tissue and the cornea is a more rigid tissue, the rate of deformation of the eyelid should be faster than that of the cornea. It is proposed that before preconditioning, the eyelid will react as a spring in response to increasing force. Since force is proportional to IOP which is proportional to volume deformation, the

applied force to applanate the cornea should be proportional to the indentation depth cubed[21]. As the cornea becomes compressed, increasing force will result in a smaller indentation.

The point on the curve marked D_1 indicates the point at which the applanation device begins to flatten the cornea. D_1 should correspond to a discontinuity in the force-indentation curve. The force corresponding to D_1 is F_e. In order to determine F_t, it is necessary to determine the point D_2 at which the cornea is completely applanated the area A_c. As discussed in Section 2.1, it is proposed that the eyelid will not further compress once corneal applanation begins, and, thus, the distance d between D_1 and D_2 is not dependent on the eyelid and can be determined by geometry as depicted in Figure 2.2.

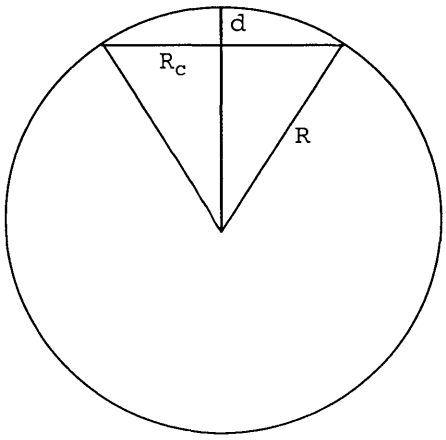

Figure 2.2: Applanation geometry of the cornea.

The distance d needed to flatten the cornea, A_c, depends on the internal radius of curvature of the cornea by

$$d = R - (R^2 - R_c^2)^{\left(\frac{1}{2}\right)}$$

where R_c is the radius of the area A_c. D_2 can then be determined by

$$D_2 = D_1 + d$$

Once D_2 is calculated, F_t can be read off the force-indentation curve, and the IOP can be calculated using the pressure relation derived above.

Thus, in order to determine the IOP of the eye by applying a force through the eyelid to the cornea, only the radius of curvature of the cornea and the force-indentation curve of the eyelid and cornea is needed. The radius of curvature of the cornea can be non-invasively determined using a Keratonometer, a clinical device found in most optometrist offices. A device capable of accurately measuring applied force and indentation distance is need to acquire the force-indentation curves.

2.3 Ultrasound Method

An alternate method for determining the forces, F_t and F_e, necessary to calculate the IOP requires a 3d graph of the ultrasound pulse echo of the eyelid and cornea indented over time plotted versus measured force. An idealized 3d graph of the positive envelop of each echo is depicted in Figure 2.3 from two viewpoints. The 4 peaks in order from left to right represent the initial pulse, the probe tip/eyelid interface, the eyelid/cornea interface, and the back of the eye. Only 12 potential scans are graphed. Had more scans been included, the echos would be more continuous with increasing force.

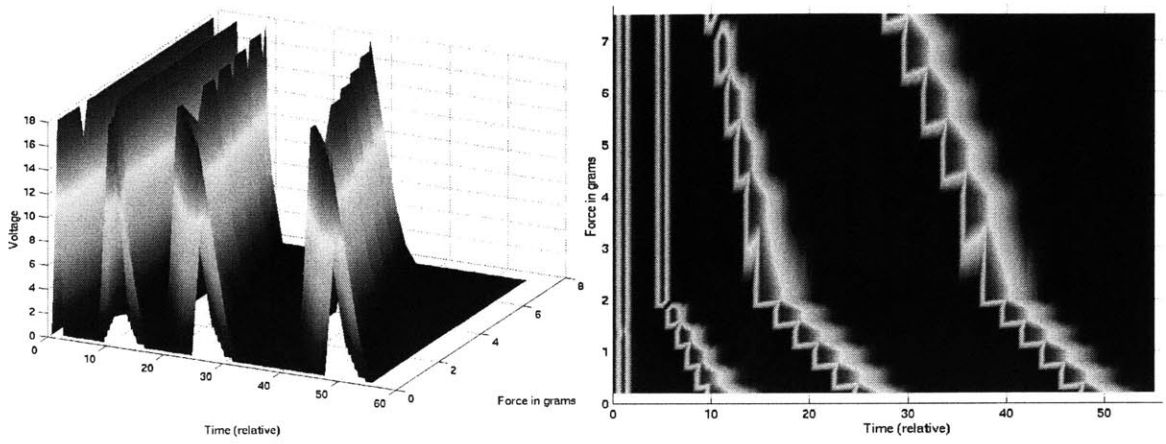

(a) (b)

Figure 2.3: Two views of an idealized 3d plot of ultrasound echos of the eyelid and cornea indented slowly over time plotted versus measured force.

As Figure 2.3b shows, the point at which the eyelid is completely applanated the area of the ultrasound probe is indicated by the narrowest width of the probe/eyelid interface echo. This point corresponds to the beginning point for corneal applanation. The point at which the cornea is completed applanated the area of the indenting probe should correspond to the narrowest width of the eyelid/cornea interface echo. The forces associated with these two points correspond respectively to the forces, F_e and F_t, required by the pressure relation derived above.

It is proposed that given such a 3d graph of ultrasound scans versus time and measured force, a trained eye could determine the applanation forces necessary to calculate IOP. This IOP determination method requires a device with an ultrasound transducer probe and force transducer to acquire the data necessary to create the 3d plots.

Chapter 3

Force Indentation Technique

3.1 Overview

In order to evaluate the viability of the first proposed through-the-eyelid tonometry technique, it is critical to determine whether the beginning point of corneal applanation can be determined from a force indentation curve of the eyelid and cornea in series. It is unnecessary to build a through-the-eyelid tonometer to make the determination. Instead, a similar, previously built device which characterizes biological tissues can be used. The device must be capable of acquiring the portion of the force indentation curve with the beginning point of corneal applanation can be used. Mark Ottensmeyer completed the device called the TeMPeST (Tissue Material Property Sampling Tool) for his Ph.D. thesis in Mechanical Engineering at MIT in February of 2001[14]. The device is designed as a minimally invasive instrument for in-vivo measurement of solid organ mechanical impedance.

3.1.1 Specifications

The TeMPeST applies a small amplitude deformation with a 5mm diameter probe to the surface of a tissue and records the applied force and probe position. The device has a range of motion of +/- 0.5mm from its starting location and can apply up to 30.6 grams of force. In order to ensure that the portion of the force indentation curve necessary to determine the beginning point of corneal applanation is acquired, a preload can be applied to partially indent the eyelid before probe movement begins. The capability and availability of the device made it the optimum choice for evaluating the viability of the first through-the-eyelid tonometry technique.

3.1.2 Functional Components

The TeMPeST is made up of several components necessary for tissue displacement and force response measurements as well as methods for applying tissue deformations. Figure 3.0 shows the sensor and actuator components of the device

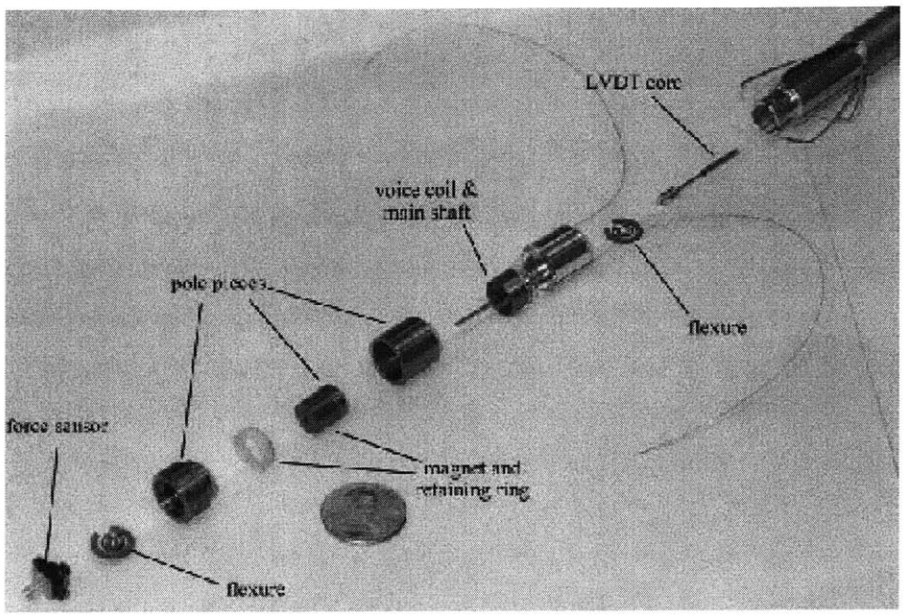

Figure 3.0: TeMPeST functional components[14].

The 5mm diameter probe and force sensor are located at the tip of the device. The voice coil actuator which converts electric current to an applied force, causing the probe tip to move, is located farther up the shaft. The LVDT (linear variable differential transformer) core which measures probe position is located near the base of the shaft.

3.1.3 System Components

The sensors and actuators are packaged in a flexible and portable arm to allow for movement and positioning of the device. Device control and data acquisition is achieved by a PC interface through an STG (Servo To Go, inc.) eight channel motion controller card. Figure 3.1 shows the system components.

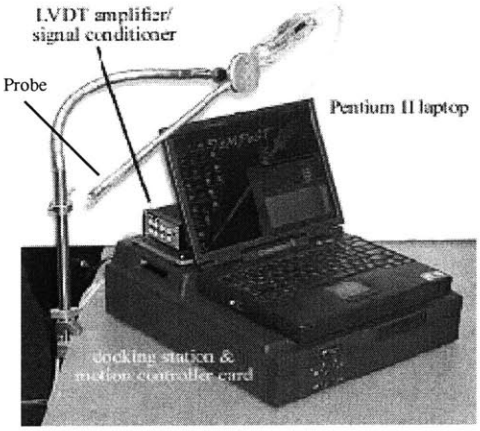

Figure 3.1: System Components[14].

A Matlab graphical user interface, in conjunction with a C++ console application, allows for real-time device control and data acquisition and display. Data acquisition options include the type, amplitude, sampling rate, and duration of the probe motion signal. Once data has been acquired, the user can choose from several data analysis and display options including both frequency and time domain analyses.

3.3 System Tests

Before running tests on the eyelid and cornea, a test was run on the forehead to ensure that the system was working properly. The skin on the forehead is soft and should be easily compressed while the bone underneath is nearly incompressible. The forehead should result in a force-indentation curve with an obvious discontinuity when the probe attempts to compress the bone.

All subsequent eye tests were run on a female subject, age 22, with normal eyes and eyelids laying face up on a hard surface with her head stabilized in a triangle shaped head rest to limit mobility. The TeMPeST probe was positioned over the right eye. The subject was instructed to keep her eyes completely closed while positioning her cornea underneath the probe. Two types of signals were used to move the probe tip: chirp and sinusoid. The chirp tests were used to evaluate the frequency dependency of the eyelid and cornea. The sinusoid tests were used to evaluate the ability to determine the beginning point of corneal applanation from force and probe position information.

3.1 Forehead Test

The preliminary forehead test was run with a sinusoid of amplitude 210mN and a preload of 84mN. Probe position versus measured force is plotted in Figure 3.2.

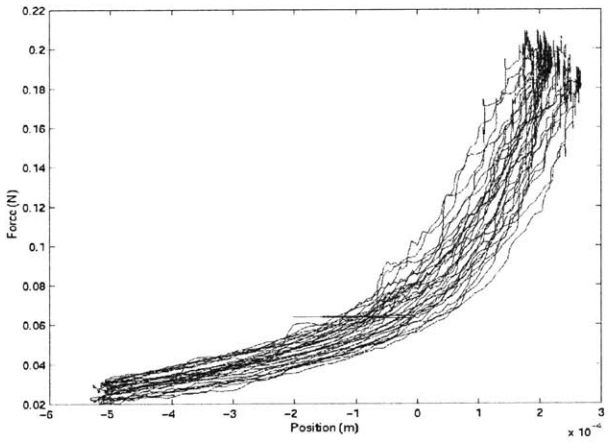

Figure 3:2 Forehead force-indentation curve.

The beginning linear portion of the graph corresponds to the probe indentation of the skin on the forehead. Once the skin has been compressed and the probe attempts to indent the bone, the force curve becomes

nearly vertical. The probe which moves +/- 0.5 mm from its starting point is unable to compress the bone, indicated by the position measurements which only go up to 0.25mm beyond the starting position. The results exhibit considerable drift, most likely resulting from slight slipping in the arm fixture or other internal irregularities in the device itself.

3.3.2 Frequency Dependency

In order to test the frequency dependency of the eyelid and cornea, 7 tests were run using a chirp signal with frequency increasing exponentially over 32.8s with a 1kHz sampling rate. Probe set-up values and resulting stiffness measurements are shown in Table 3.0. For each test the amplitude and preload were set to test either the eyelid or cornea separately, however, the subject often reported inaccurate placement of the probe. Thus, the subject's assessment of what tissue was being indented during each test is reported in the table.

Data Set	Amplitude (mN)	Preload (mN)	Freq. Range (Hz)	Stiffness (N/m)	Tissue Indented
1	30	30	0.1-10	20-40	Eyelid
2	30	30	0.1-10	20-40	Eyelid
3	30	120	0.1-10	30-50	Eyelid
4	30	30	0.1-50	60-100	Eyelid/ Cornea
5	30	120	0.1-10	60-80	Eyelid/ Cornea
6	90	90	0.1-20	70-180	Mostly Cornea
7	30	120	0.1-10	100-150	Cornea

Table 3.0 Frequency dependency tests set-up values and stiffness results.

The results show increased stiffness with increasing rate of indentation for both the eyelid and cornea individually and in series. The range of stiffness values were characteristically larger for the cornea than for the eyelid, suggesting that the cornea is more frequency dependent than the eyelid. The eye is filled with fluid in both a liquid and gel form which most likely causes the frequency dependency. Under low frequency applied force, the fluid in the eye can slowly compress or flow out of the eye resulting in a low stiffness. Force applied at a higher frequency will result in higher stiffness numbers since the fluid in the eye will resist rapid outflow and compression.

3.3.3 Force Indentation Curves

Nine experiments were run to obtain force indentation graphs of the eyelid and cornea both independently and in series. The TeMPeST operator attempted to position the probe in the exact same location for every test. All measurements are 0.5Hz sinusoids sampled at 500Hz and duration of 32.8s. Preload forces and amplitudes were chosen to obtain the three types of force curves. Table 3.1 shows the setup values and measured stiffness values.

Data Set	Amplitude (mN)	Preload (mN)	Stiffness (N/m)	Tissue Indented
1	30	30	43.07	Eyelid
2	30	30	41.82	Eyelid
3	30	30	38.0	Eyelid
4	90	45	32.15	Eyelid
5	90	45	47.44	Eyelid
6	210	84	65.30	Eyelid/Cornea
7	207	90	68.27	Eyelid/Cornea
8	240	30	80.67	Eyelid/Cornea
9	150	120	94.83	Cornea

Table 3.1: Sinusoid tests set up values and stiffness results.

Tests 1-3 were intended to test the eyelid alone, 4-8 the eyelid and cornea, and 9 the cornea alone. The subject indicated that tests 4 and 5 only indented the eyelid. She also described the difficulty of keeping her eyelids closed while positioning her cornea under the probe tip. In most cases she was unable to keep her eyelids and cornea from moving for the entire duration of a test. The subject noticed that the probe often slipped slightly from its starting position during a test.

Eyelid tests resulted in the lowest stiffness values, the cornea test the largest. Tests in which both the eyelid and the cornea were indented resulted in intermediary stiffness values. These stiffness values support the proposal that the eyelid is a more easily compressible tissue than the cornea.

Figure 3.3 shows the probe position plotted versus force for data sets 5,6,8 and 9. Each data set exhibits considerable drift which may be caused by the slight slipping of the probe as reported by the test subject. Drift was also exhibited in the forehead test, suggesting eyelid or corneal movement is not the cause.

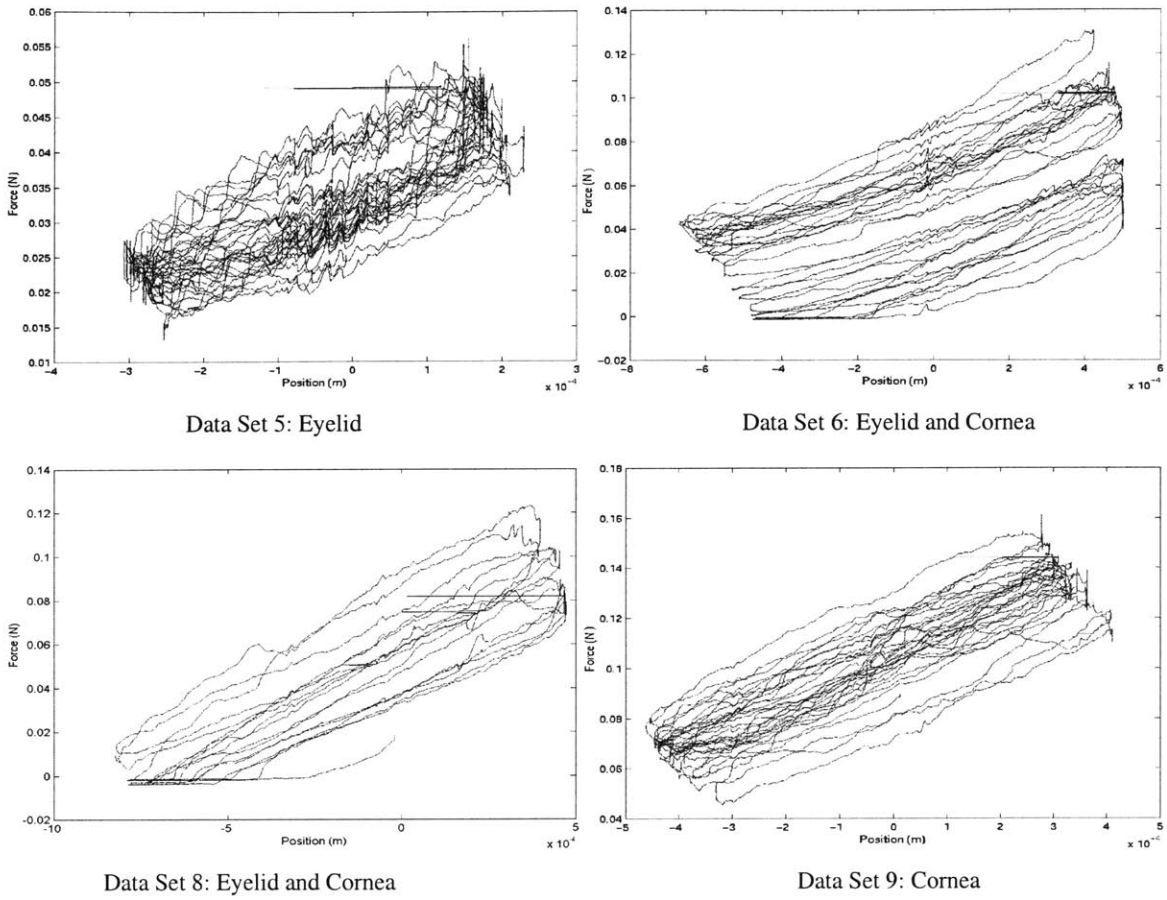

Data Set 5: Eyelid

Data Set 6: Eyelid and Cornea

Data Set 8: Eyelid and Cornea

Data Set 9: Cornea

Figure 3.3: Force-indentation curves for data sets 5, 6, 8 and 9.

As expected the curve for the eyelid is fairly linear with irregularities, most likely attributable to eyelid flutter. Data sets 6 and 8 were the only two eyelid/cornea tests in which the probe moved from completely not touching the eyelid to indenting both the eyelid and cornea. These curves appear to be slightly nonlinear with a small discontinuity that may be due to the stiffness differences between the eyelid and cornea. The force curve of the eyelid and cornea for data set 7, not shown, appeared completely linear. The cornea indentation results of data set 9 exhibit linear indentation depth versus applied force, which does not correspond with the expected quadratic curve as discussed in Section 2.2.

Chapter 4

Ultrasound Technique

4.1 Overview

In order to evaluate the viability of the ultrasound through-the-eyelid tonometry technique, an ultrasound/ force measurement system was built. The system consists of an ultrasound transducer, which acts as an indentation probe, attached to a force transducer which measures the applied force of the probe. The system is depicted in Figure 4.0. A skilled device operator is required to position the probe and to apply all indentation forces. The device operator slowly increases the probe indentation force to the eyelid and cornea until a force sufficient to applanate the cornea the area of the probe is surpassed. As this slow indenting process occurs several ultrasound echos and corresponding force measurements are acquired. A 3d plot of the ultrasound echos versus force is generated and displayed on a PC. As discussed in Section 2.3, it is expected that the eyelid/cornea interface echo will reduce in width as the cornea is flattened.

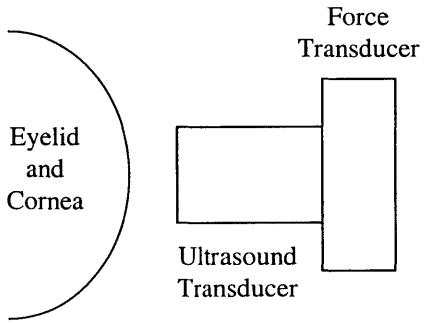

Figure 4.0: Device Components

4.1.1 Specifications

Because the ultrasound system is being used for evaluation and not for actual IOP measurements, system specification are not as stringent as those for a clinical tonometer. A clinical tonometer should have a probe tip comparable in diameter to the standard Goldmann tonometer (3.06mm) for minimal corneal indentation. As discussed in section 1.2, the smaller the deformation, the less prominent are errors due to varying mechanical properties of the cornea. The force transducer must be capable of measuring pressures from 0mmHg to 60mmHg with sub 1mmHg resolution. The ultrasound transducer must have good near-surface resolution and thin thickness gauging capabilities. Rigorous signal processing of the ultrasound echos should be unnecessary for evaluating the viability of the tonometry technique. The ability to observe the trends described in Section 2.3, rather than determining exact distances, is most important.

If an ultrasound tonometer is put into clinical use, data should be accurately displayed real-time in a 3d plot of ultrasound echo versus measured force. A trained technician could use the real time scans to position the probe and to determine when applanation has occurred and further measurements are unneeded. For the explorative nature of this project, 3d plotting is only required as a post data acquisition processing step.

4.1.1 System Components

Figure 4.1 shows the ultrasound/force measurement system, which consists of 4 main components. As its name describes, the pulse generator (pulser) generates the signal to initiate the ultrasound pulse and to command the oscilloscope to begin recording the force transducer output and the ultrasound echos. The ultrasound transducer converts the electrical pulse into a sound wave. Reflections are converted back into electrical signals which are received by the pulse receiver and relayed to the oscilloscope as a radio frequency.

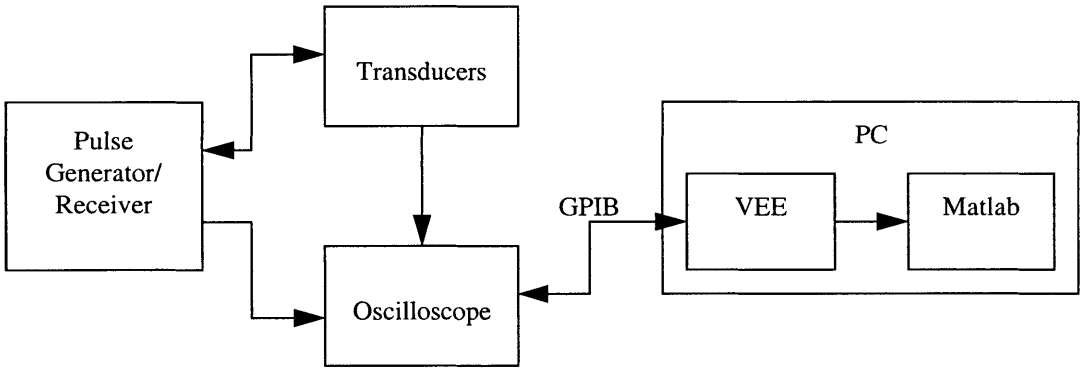

Figure 4.1: System block diagram.

A user interface created in Agilent VEE 5.0 software resides on the PC. The VEE program, which controls oscilloscope initialization and data acquisition, communicates with the oscilloscope over a General Purpose Information Bus (GPIB) interface. Approximately one ultrasound scan is received per second. The oscilloscope must receive and implement its initialization commands as well as receive a start signal from the VEE program before it acknowledges the pulse generator's signal to record data. Once all the data has been recorded, a Matlab script can be executed to generate a 3d plot of the data.

4.2 Details

The ultrasound/force measurement system is divided into three sections: hardware, data acquisition, and PC interface. Hardware includes the force and ultrasound transducers, data acquisition includes the pulse generator/receiver and the oscilloscope, and the PC interface includes a program capable of controlling data acquisition and display through a user interface.

4.2.1 Hardware

The system hardware shown in Figure 4.2 includes the transducers which interface between the ultrasound system and the eyelid and cornea. The force transducer is situated in a groove dug out of a metal strip. The ultrasound transducer, which acts as the indentation probe, is then mounted on top of the edges of the metal strip directly above the force transducer. The metal strip acts as a grip for the device operator. The force exerted by the eyelid and cornea back onto the indenting probe is measured by the force transducer.

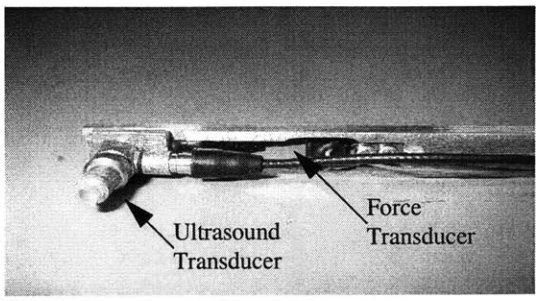

Figure 4.2: The ultrasound transducer and force transducer mounted to a metal grip.

The 20MHz Panametrics Videoscan Delay Line Transducer shown in Figure 4.3a was chosen as the contact ultrasound transducer due to its good near-surface resolution and precision thickness gaging. The transducer is 3mm in diameter with a 6mm diameter probe, which necessitates a change in the area, A_a, in the pressure equation in Section 2.1 from 7.35mm^2 to 28.27mm^2. Using this probe area, 10mmHg will correspond to a reading of 3.84 grams of force.

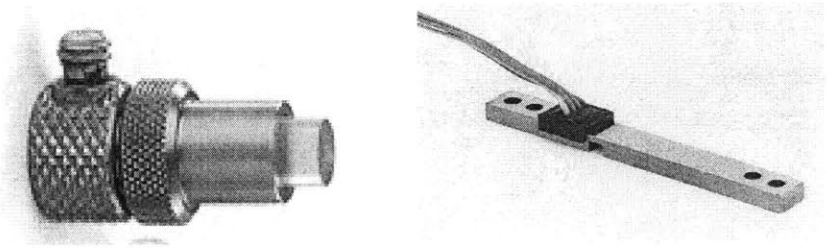

(a) Ultrasound Transducer (b) Force Transducer

Figure 4.3: Ultrasound system functional components.

When the transducer receives a start pulse from the pulse generator, a longitudinal sound wave is produced. The delay line allows the transducer to cease vibrating before receiving reflections. The resulting ultrasound scan will have multiple echos from the end of the delay line. It is necessary to put water or electrolyte gel between the transducer and the delay line and between the delay line and the test object to facilitate sound wave propagation.

The SMD S100 Cantilever Beam Load Cell shown in Figure 4.3b was chosen as the force transducer. This load cell has a 50 gramf capacity, a maximum deflection of 0.89mm, a hysteresis of 0.03% R.O. and a non-repeatability of 0.05% R.O.

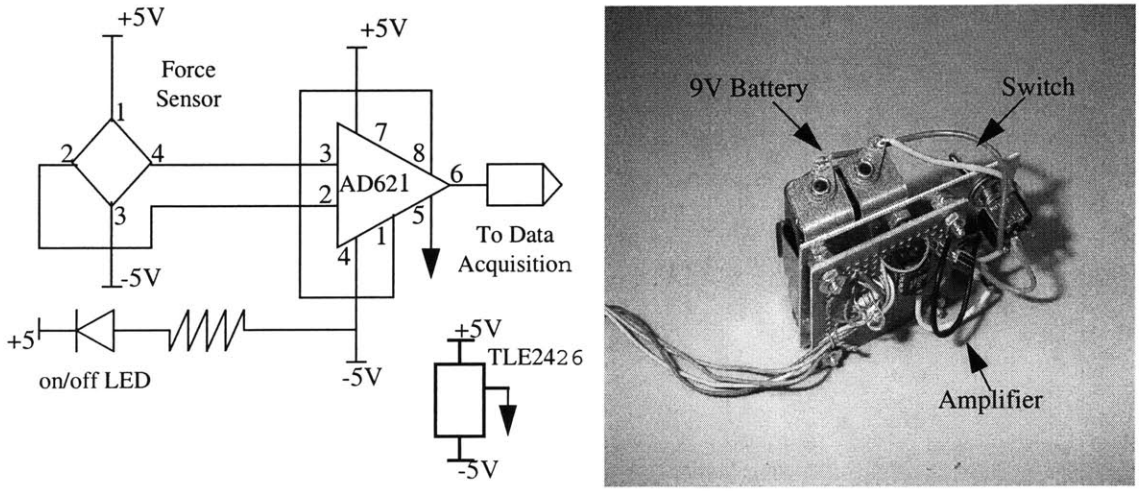

Figure 4.4: Force sensor amplification circuit.

The forces measured by the ultrasound system are amplified 100 times by the circuit shown in Figure 4.4. A 9V battery is used to power the circuit. The measured forces are fed into the AD621 differential amplifier, amplified 100 times, and then transmitted to the oscilloscope.

4.2.2 Data Acquisition

There are two sources of data in the system, a force transducer and an ultrasound transducer. The Panametrics ultrasonic pulse/receiver model 5072, depicted in Figure 4.5, controls data acquisition from the ultrasound transducer. The pulser generates short, large-amplitude electric pulses. When applied to an ultrasound transducer, the electric pulses result in short ultrasonic pulses and, when applied to an oscilloscope, acts as a trigger for data acquisition. The echos received by the ultrasound transducer are amplified by the receiver and are output to the oscilloscope as radio frequencies. The appropriate energy, damping, gain and bandpass values must be chosen to obtain the optimum results. The highest energy level was chosen to increase echo width and a low damping level of 50 Ohms was chosen since the transducer's delay line already damps the signal. Gain values and bandpass values were chosen based on individual experiments.

Figure 4.5: Ultrasound pulser/receiver

In order to facilitate the communication of analog signals to the PC interface, a Hewlett Packard 1663AS logic analyzer/oscilloscope is used. The oscilloscope has two input channels to receive the ultrasound echos and force measurements. These channels can sample at 1 GS/sec with a 250MHz bandwidth and use an 8 bit real-time A/D converter. The oscilloscope has an external trigger input to receive the pulser signal and a GPIB port for PC communication.

4.2.3 PC Interface

A PC fulfills three essential functions in the ultrasound/force measurement system: oscilloscope control, data acquisition, processing and display, and user interface. The first function involves sending configuration commands to the oscilloscope over GPIB, signaling the oscilloscope to begin sampling, and recording the ultrasound echos and force measurements input to the oscilloscope channels. The processing and display function involves computational functions and visual tools for 3d plotting of the recorded data. The third function allows the user to start and stop data recording and display.

In order to fulfill the above requirements, the PC must have the following features: a GPIB card, Windows 98 or NT or higher, a 380 MHZ processor or higher, 192 MB RAM or higher, Agilent VEE 5.0 with HP I/O configured, and Matlab R11 or higher. The color scheme on the monitor should be set low, 256 colors, to improve 3d plotting time. RAM disks and other Windows configuration tweaks did not improve 3d rendering time significantly.

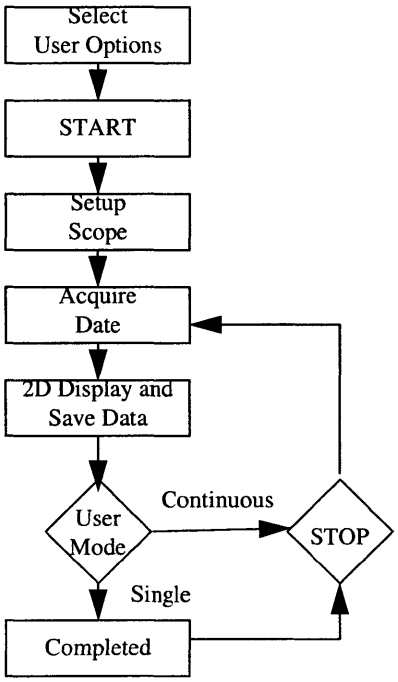

Figure 4.6: Flow chart of VEE program.

The user program that controls oscilloscope configuration and data storage and display was created in Agilent VEE 5.0, a visual programming environment for creating instrument control applications. The ultrasound system program is found in the file ViewScope.vee and implements the flow chart in Figure 4.6. Some of the code was stripped from a similar program written by Ryan Carlino for his Master's thesis completed for MIT in 2000[2].

First the user selects the user options on the GUI and presses start. The program then configures the scope and retrieves the data. Once all the data for the current ultrasound scan has been acquired, the data is saved. If the continuous scan user option is chosen and stop has not been pressed, control is passed back to the acquire data block and the process continues until stop is pressed. If the single scan user option was chosen, the program halts data acquisition. The matlab script make3dplot.m to create a 3d plot of the data is executed independently of the VEE program. See Appendix A. If further system development necessitates the matlab script be called from within the VEE program, an upgrade to Agilent VEE 6.0 should be made.

Upon opening the VEE program, two essential program views are available: the user interface view, and the program view. One of two of these views will automatically be loaded when the program is opened. In the upper left hand corner of the program window, there are two small icons which when clicked allow the user to switch program views.

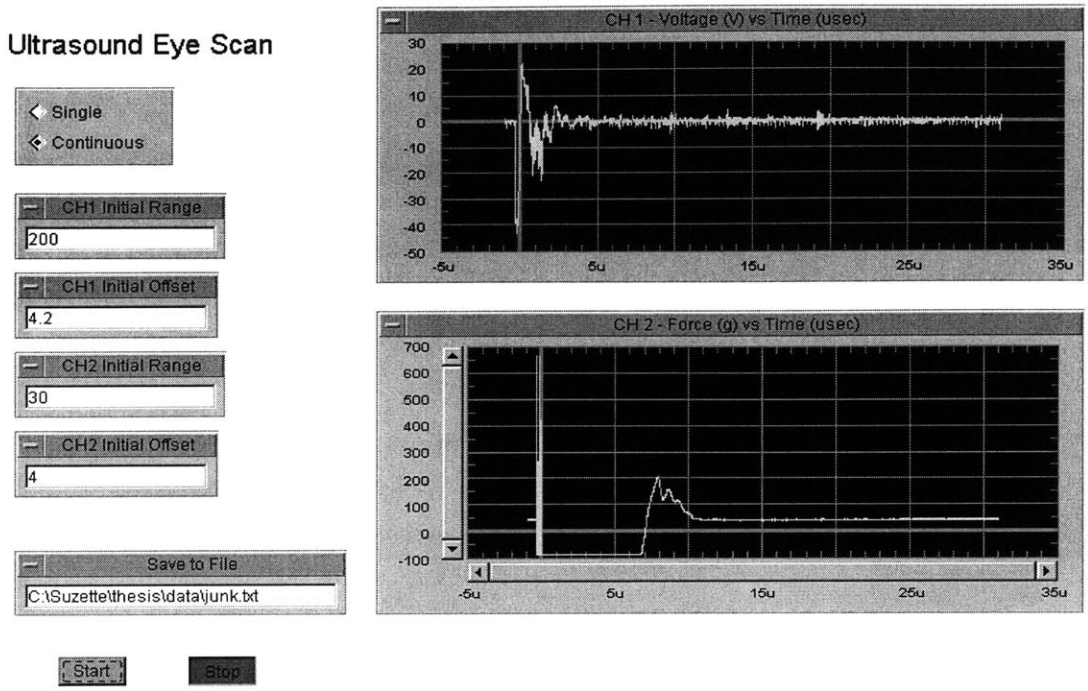

Figure 4.7: User Interface

The user interface shown in Figure 4.7 has very few elements. The user options include choosing between doing a single scan and doing continuous scans, setting CH1 and CH2 ranges and offsets, and a text box to input the file path to which data should be recorded. Once the options have been chosen, the user can click the start button to begin the scanning process. If the continuous option is chosen, the user must click the stop button to cease scanning. As each ultrasound scan and corresponding force measurement is received by the VEE program, their waveforms are displayed in the two graphing areas on the user interface. If a VEE 6.0 upgrade is made and the program calls the matlab script to generate the 3d plot, the plot should not be displayed in the user interface. Instead, the 3d plot should pop up in a separate window on the computer monitor. It is possible to save the 3d plot and have an image in the user interface that will display the 3d plot from file. However, the resolution of the 3d images when saved and subsequently viewed in the user interface is significantly degraded.

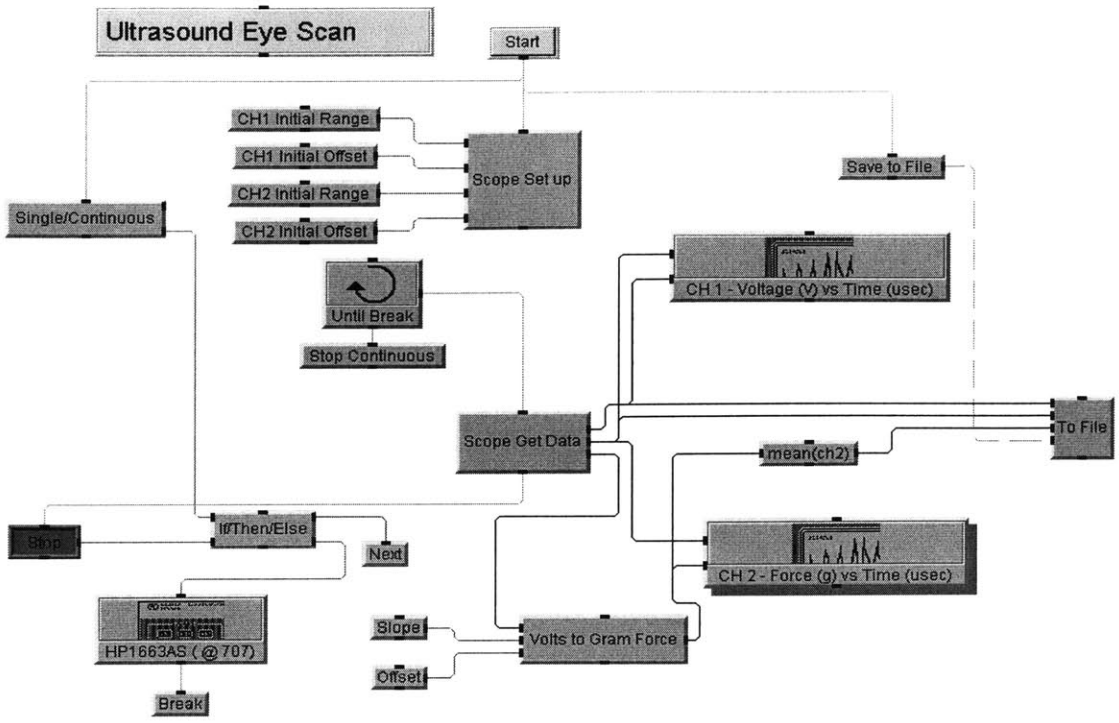

Figure 4.8: Program data flow diagram.

A data flow diagram of the entire program is shown in Figure 4.8. In most cases, lines originating from the sides of modules indicate data flow from left to right and lines originating from the bottoms of models indicates control flow from top to bottom. Once the start button is clicked, control passes to the user options and scope set up. The channel options are data inputs to the Scope Setup, a module which configures the oscilloscope. Once the setup completes, the program enters a loop indicated by the Until Break block. Control now passes to the Scope Get Data module which retrieves the data from the current ultrasound scan and force measurement. The force voltage is converted to units of gramf by the Volts to Gram Force module and data is then passed on to the Mean and Waveform blocks. The Mean block calculates the average force measurement retrieved over the course of a single scan. The Waveform blocks graph the ultrasound scan and the force measurements. All of the data is passed on to the To File module where it is saved to the file chosen by the user. After the Scope Get Data block completes, control passes to the If/Then/Else block which determines whether another scan should be made. If the stop button has not been clicked and the user has chosen the continuous scanning option, control passes to the HP1663AS block which performs direct I/O with the oscilloscope. The block instructs the oscilloscope to begin running again, and the Until Break loop continues. If the stop button is clicked or the user has chosen a single scan, the program halts. The matlab script can then be executed to generate a 3d plot of the recorded data.

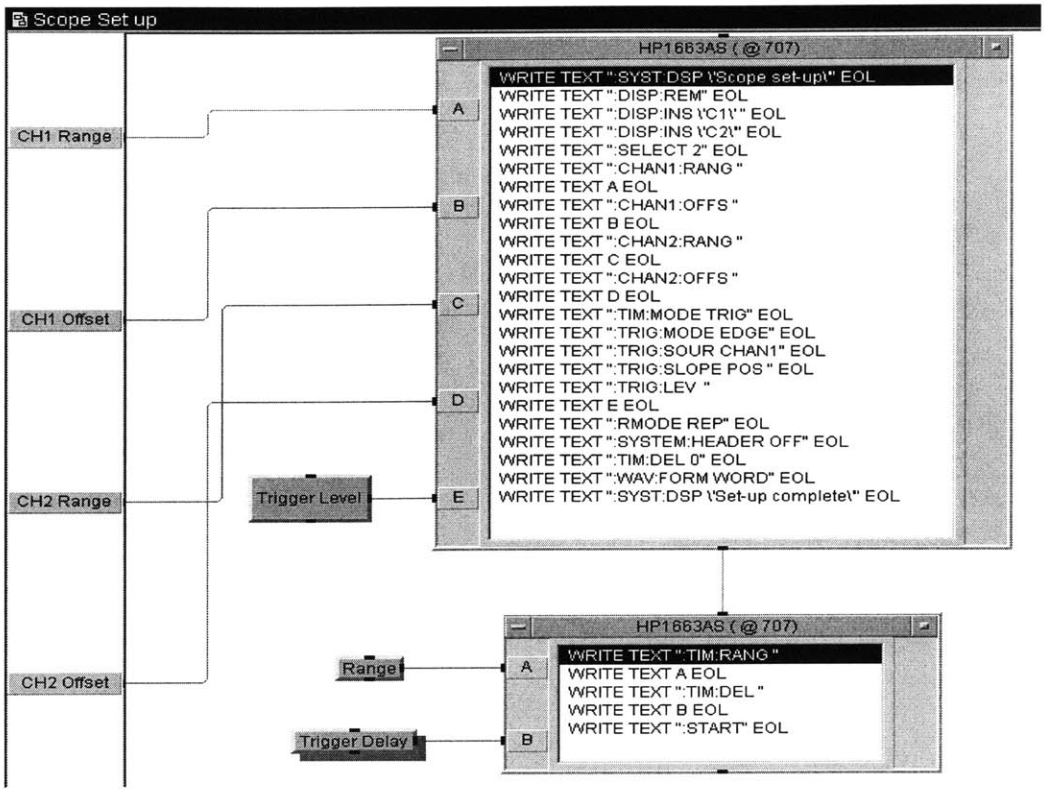

Figure 4.9: Scope Setup Block

The two modules, Scope Setup and Scope Get Data, require closer inspection. Figure 4.9 details the Scope Setup block. The main module is the HP1663AS module which contains the configuration commands sent to the oscilloscope. The configuration commands are dictated by the channel and time ranges and offsets and trigger levels and slopes. Channel 1 is used to record the ultrasound scan and Channel 2, the force measurement.

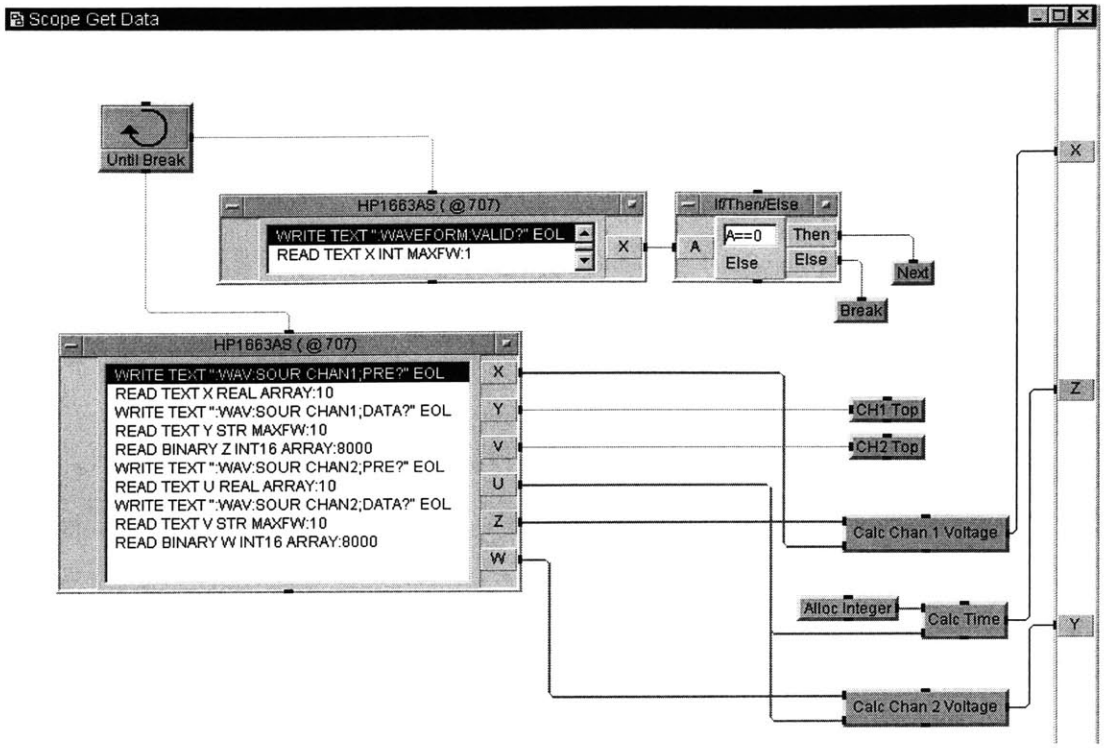

Figure 4.10: Scope Get Data Block

Figure 4. shows the details of the Scope Get Data block. There is an Until Break loop at the top of the module. When the oscilloscope has valid waveforms, the break condition is met, the loop halts, and control passes to the large HP1663AS module. The module requests the preamble and the 8000 data values which are 15-bit integers from the oscilloscope. The preamble contains information to convert the 15-bit integers data values to voltages. These conversions are made and the time axis is create. The VEE program captures approximately 1 ultrasound scan per second.

4.3 System Tests

The experimental setup is shown is Figure 4.11. Due to the slow scan/second data acquisition rate, it was necessary to choose a setup which would allow the user to move the probe in micrometer increments.

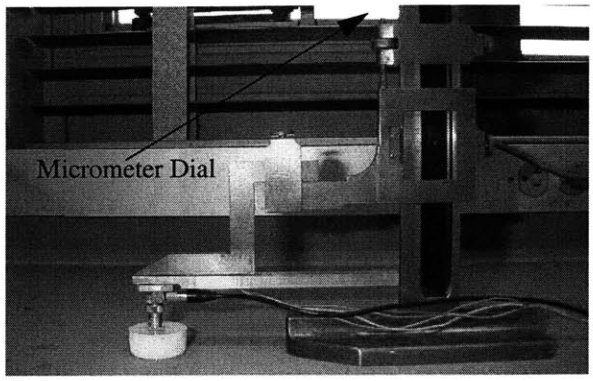

Figure 4.11: Experiment Setup

The probe is attached to the arm of a standing machinist's micrometer which can be positioned over a test object. Once in place incremental movements of the probe in the vertical direction can be made by slowly turning the micrometer dial. Test objects are attached to the bottom of a plastic bottle cap filled with water.

4.3.1 Force Calibration

The force transducer must be calibrated to determine the slope and offset values necessary for conversion of measured force to grams. Although a precise force calibration method is desired for exact tonometry readings, a rougher process is adequate for the purposes of the evaluation tests. Stacks of 0 to 8 nickels were placed on top of the system probe as shown in Figure 4.12a.

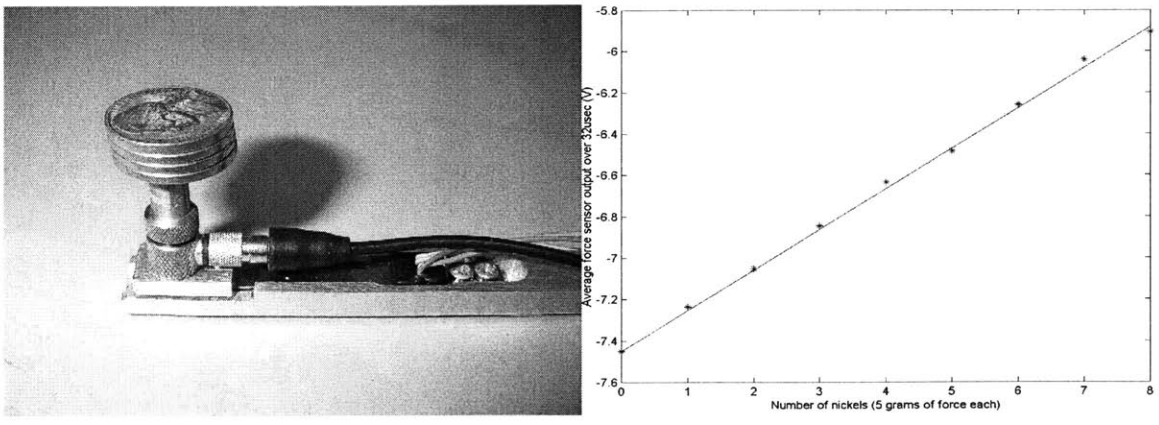

(a) (b)

Figure 4.12: Force calibration with nickels.

As discussed in Section 4.2, the set of force sensor readings for each ultrasound scan is averaged by the VEE program since only one force need be associated with a particular scan. For each average force recorded during calibration, the corresponding set of force readings showed between 96.6 and 98.3% correlation. These average forces are graphed versus the number of nickels on the system probe in Figure 4.12b. Since each nickel weighs approximately 5 grams, the slope of the line of best fit is 0.196, and the y intercept is -7.45, average force outputs should be multiplied by 25.5 and added to 7.45 to obtain force units of grams. Calibration must be repeated before each use, and the slope and offset values updated in the VEE program.

4.3.2 Distance Calibration

Before exploring the potential uses of ultrasound for determining the curvature of a surface, it is first necessary to look at the initial ultrasound pulse and to ensure that the transducer is capable of recording differences in distances between the probe's tip and a flat surface. Figure 4.13 shows the initial ultrasound pulse which extends from 1.7 to 2.5 us.

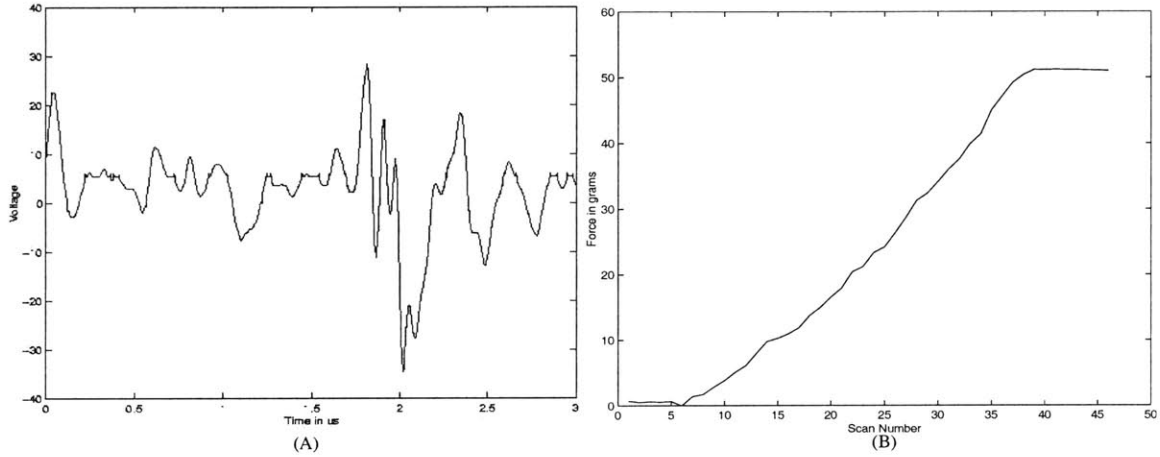

Figure 4.13: (A) Initial ultrasound pulse waveform. (B) Force curve of the probe with attached spring being lowered into a bottle cap full of water.

Figure 4.13b shows the results of the probe with an attached spring being slowly lowered into a bottle cap full of water. The scans before the spring touches the bottom of the bottle cap result in essentially 0 grams of force readings. Once the spring touches, the force measurements ascend linearly as the spring compresses until the maximum force capacity of the force transducer is reached. The linear accuracy of the graph is dependent on the user's ability to turn the micrometer dial uniformly and the uniformity of the spring.

Figure 4.14 shows two views of the 3d plot of scans 6 through 38 versus measured force. The first view is an angled 3d view, and the second view looks down onto the first view from the top. The left-most diagonal line at time 1us in the second view is the echo made by the bottom of the bottle cap. Subsequent diagonal lines are repeated echos. The lines move backwards in time with increasing force since increasing force indicates that the spring is compressing and the probe tip is getting closer to the bottom of the bottle cap, and, thus, echos of the bottom have a shorter distance to travel to the ultrasound receiver.

.

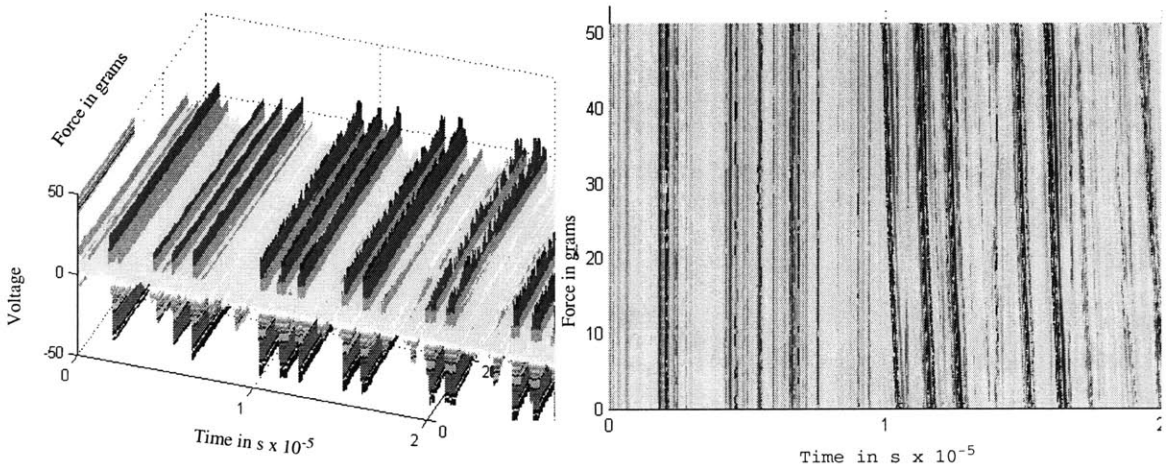

Figure 4.14: 3D plot of probe moving towards bottom of bottle cap using a spring to obtain changes in force readings.

Eight spring tests were performed with two springs of differing compressibility in order to determine the time on the ultrasound scan where an echo for a surface touching the probe would be situated. The probe was lowered into the bottle cap until it touched the surface. The point at which the echo of the surface ceased to move diagonally backwards in time is the time at which echos for surfaces touching the probe tip should always be situated. Figure 4.15 shows one of these spring tests. When the spring makes contact with the bottom of the bottle cap, the surface reflection is at time 3us. Once the probe touches the bottom of the bottle cap, the reflection is at time approximately 2us. The average time of the echo for probe/ surface contact over the 8 tests occurred at 2.1us.

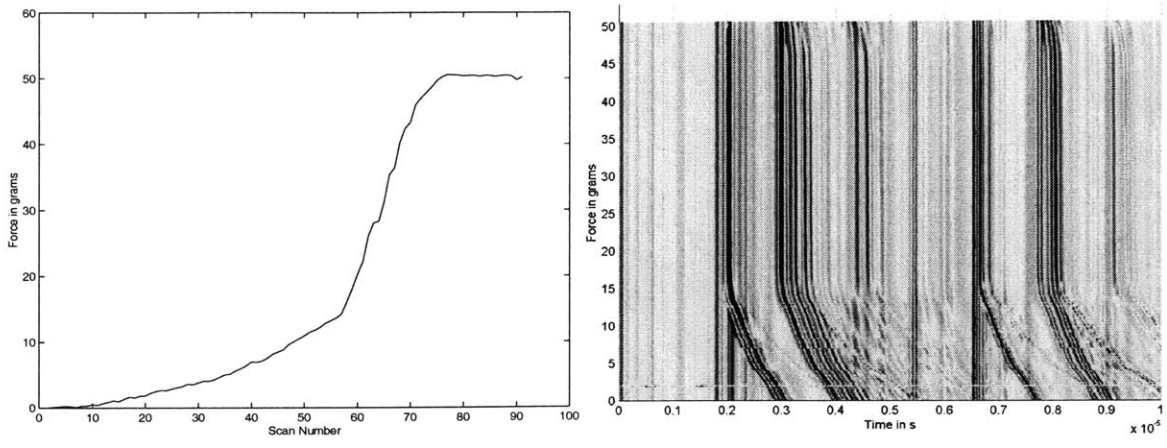

Figure 4.15: Results of the probe with attached spring being lowered into a bottle cap full of water until probe/bottle cap contact is made.

Since recognizing corneal applanation requires being able to distinguish sub-millimeter distances, it is useful to relate time in the ultrasound scan to distance. Twelve 2 tests with two springs of differing compressibility were run in which the probe with the attached spring was lowered 1mm into the bottle cap. The time difference between the beginning and the end of the diagonal echo is the conversion factor between time and 1 mm of distance. The results of the 24 tests are plotted in Figure 4.16.

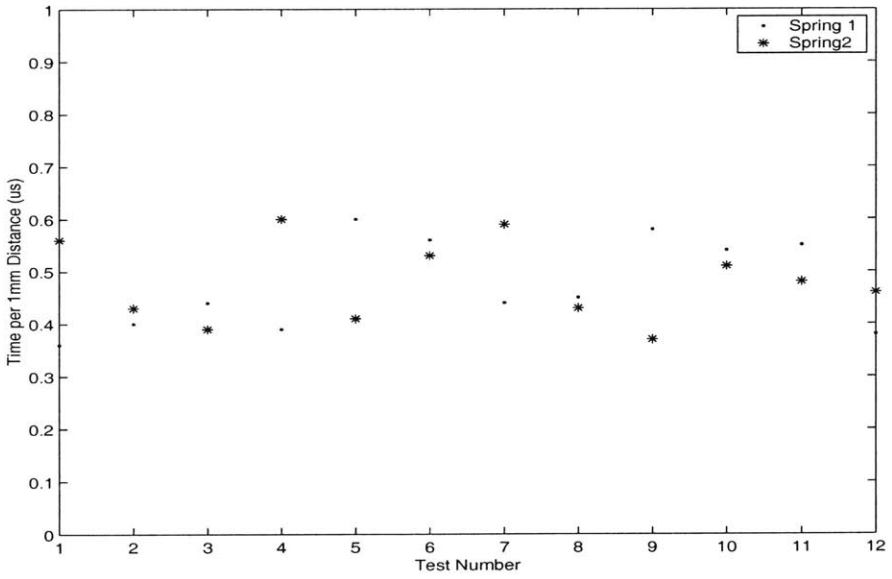

Figure 4.15: Results of relating time to distance in an ultrasound scan.

The wide range of results (0.36us to 0.6us per 1 mm of distance moved) is most likely explained by the inability of the device operator to move the micrometer exactly 1 mm for each set of measurements. Knowing an approximate relation between time and distance traversed by the probe toward a surface, however, should aid 3d plot observers in recognizing echo width changes of distances significant to corneal applanation.

4.3.3 Applanation Tests

Four applanation tests for three different hemisphere phantoms were performed. These phantoms included two rubber balls with differing stiffnesses, both with radius 17mm, and grapes with approximate radii of 10mm. Each object was cut in half and placed in the bottom of a plastic bottle cap full of water. Since the rubber balls float, they were affixed to the bottom with JB Weld, an epoxy, which when dried, minimally compresses under force.

Due to their diameters, the rubber balls and grapes should be completely applanated when they are indented a distance of 0.27mm and 0.46mm respectively. Using the distance to time relation determined above, the surface echos of the rubber balls and grapes before any indenting should have a width range of 0.1us to 0.162us and 0.166us to 0.276us respectively. These widths are expected to decrease as the curved surface is flattened as discussed in Section 2.3. Figure 4.17 shows the results of one applanation test per object. Only the scans from first contact with the surface through those just exceeding the force transducer's capacity were plotted. Results were repeatable.

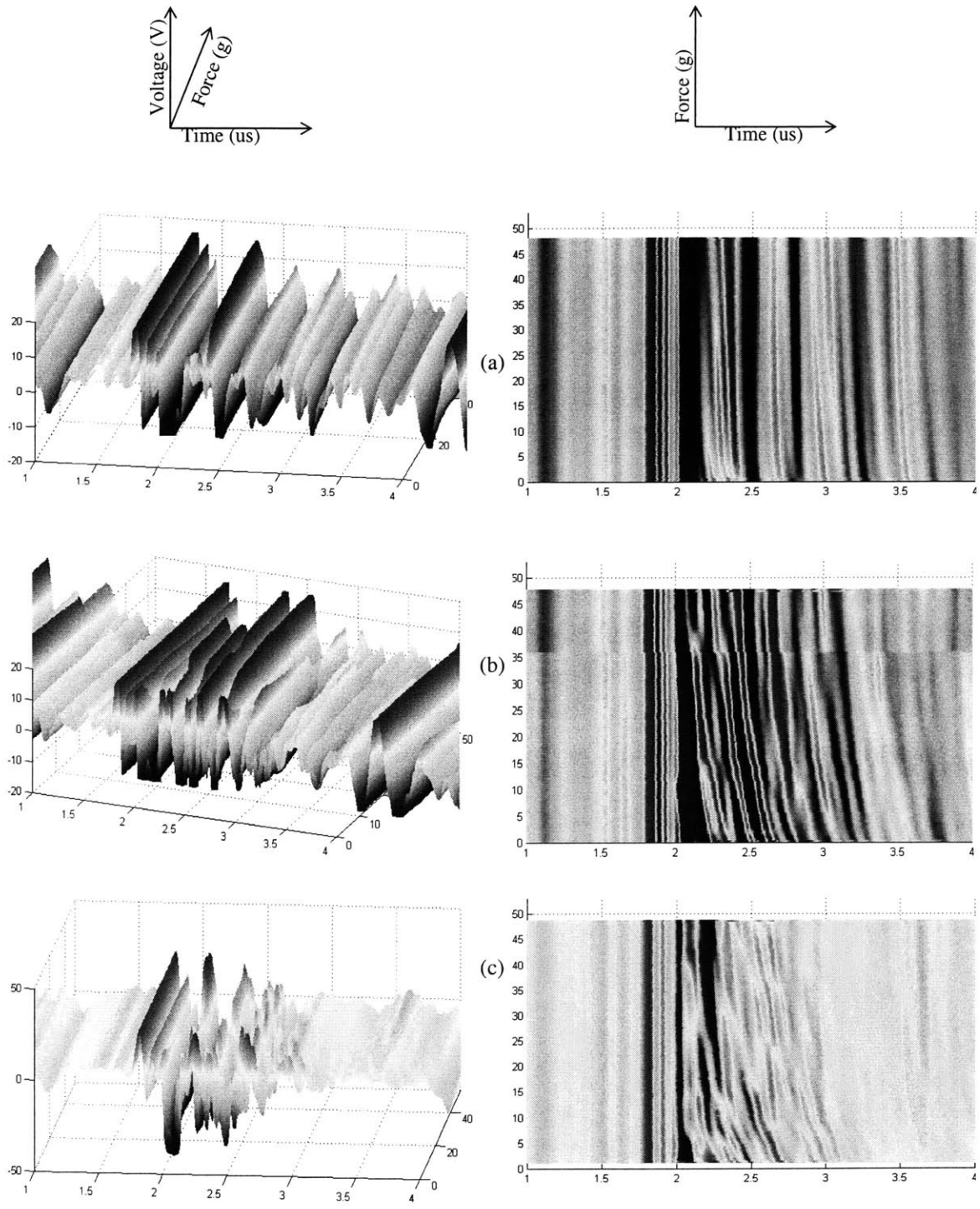

Figure 4.17: 3d ultrasound applanation plots for a (a) hard rubber ball (b) a soft rubber ball and (c) a grape.

As expected, the surface echo at the point of probe contact occurs at approximately 2.1us. The initial pulse overlaps the surface echo. We see that the echo actually moves backwards in time with increasing force for each test object even though the probe should not be getting closer to the closest point on the surface.

It is impossible to decipher how many of peaks are involved in the surface echo by sight. The expected widths of the echos gives some indication of how wide the echos should be, although there is an additional signal in the scans which complicates reading the 3d plots. The additional signal is too regular from scan to scan to be noise and is most likely some interfering radio frequency.

Because the expected trends in echo width were hard to decipher, additional measurements of the force at visible applanation of the three test surfaces were recorded. Once the hard rubber ball was applanated, the force transducer's capacity was already exceeded. The soft rubber ball applanated at a force of 35.6 gramf and the grape at 23.3gramf. Even though this information should help locate the important place in a 3d plot to look for applanation, it is still impossible to determine the force at applanation from the 3d plots acquired for any of the test objects.

During each probe use, the ultrasound transducer moves backwards toward the force transducer approximately 0.3mm as applied force is increased. Once this distance has been traversed, the probe no longer has room to move backwards and instead the test object must yield. During this time period, whether or not the test object is indented at all is dependent on the stiffness of the object. It was observed that the hard rubber ball was not indented at all while the ultrasound probe moved backwards 0.3mm. The soft rubber ball indented just slightly, and the grape indented approximately 0.2mm. The movement of the ultrasound probe backwards causes its angle with respect to the curved surface to change slightly. This movement may cause the observed diagonal movement in the surface echos. It may also obscure the ability to determine applanation in the 3d plots from surface echo width.

Chapter 5

Conclusions

Two through-the-eyelid tonometry techniques are proposed and evaluated. The results must be analyzed in order to determine whether the techniques are viable and whether future exploration is needed.

5.1 Force-Indentation Method

The force-indentation method involves determining the beginning point of corneal applanation from a force-indentation curve of the eyelid and cornea. Experiments involving the TeMPeST suggest that the eyelid and cornea do have differing stiffness values. However, the force-indentation curves obtained from 1mm eyelid/cornea indentation depths do not obviously exhibit a change in stiffness when the probe begins to flatten the cornea. Two data sets appear to exhibit a slight change in stiffness at the approximated point of complete eyelid indentation. The results also suggest that the cornea has a more significant frequency dependency than the eyelid.

Several factors may have influenced the accuracy of the results, including probe and subject movement. The flexure arm used to stabilize and position the probe slipped slightly throughout many tests, and the probe tip was difficult to position exactly. The subject found it impossible to remain completely still and fluttered her eyelids and moved her cornea often. She occasionally moved her head backwards away from the probe tip slightly during tests as well. It is also possible that even though the subject was lying down, applied force caused the eye to move back slightly into the eye socket, thereby obscuring the curves.

Future tests require a better method for probe stabilization and initial placement. Another device with a larger range of indentation would allow for less precise probe placement since the probe could be placed just touching rather than partially indenting the eyelid. Using a sinusoid superimposed on a ramp rather than a purely sinusoidal signal for position movement should help locate the discontinuity point between eyelid and corneal indentation by making the second harmonic at the discontinuity more obvious. Tests indenting both the eyelid and cornea at a higher frequency may result in a greater distinction between the stiffnesses of the cornea and eyelid as well; however, higher frequency indentations might result in measured pressures that exceed those of the Goldmann tonometer.

5.2 Ultrasound Method

The ultrasound-force tonometry technique involves recognizing applanation trends in a 3d plot of ultrasound scans of the eyelid and cornea versus increasing applied force. The ultrasound system tests on hemisphere phantoms and springs in water-filled bottle caps did exhibit the expected trends in distance changes between the probe tip and test surfaces. It was difficult to determine the width of the surface echos and impossible to recognize the expected trend in decreasing surface echo width as the surface was flattened.

The initial pulse as well as an interfering unknown signal, most likely a radio frequency, obscured the 3d plots. The backward movement of the ultrasound probe during initial contact with a surface may allow the force transducer to reach capacity before applanation actually occurs. Changes in the angle between the probe tip and the surface as the probe moves backward may also affect the accuracy of the results. The damping and energy settings may not be optimum.

The probe should be redesigned so that force readings during surface contact are only associated with surface applanation. Signal processing to isolate and remove the initial pulse as well as the unknown low amplitude signal from the 3d plots should be pursued. Additional tests to reassess the optimal damping and energy settings should be conducted.

5.3 Pressure Equation

The intent of through-the-eyelid tonometry is to reduce the discomfort caused by direct contact with the cornea in Goldmann tonometry. However, by taking measurements through the closed eyelid, a new set of potential errors are introduced. The proposed through-the-eyelid tonometry techniques attempt to avoid dependence on specific eyelid properties by using the force necessary to flatten the eyelid in IOP calculation. However, the eyelid may continue to flatten depending on the specific eyelid mechanics after corneal applanation begins. The eyelid may also exhibit a relaxation effect resulting in smaller IOP readings. Involuntary eyelid and eye movement may also cause errors in measurement. Because the eyelid is closed, ensuring accurate probe positioning over the cornea is complicated.

If future tests conclude that the through-the-eyelid techniques are viable and actual through-the-eyelid tonometers are constructed, the proposed IOP equation should be evaluated. The accuracy of the equation is prone to the discussed potential eyelid errors as well as the same sources of errors as Goldmann Tonometry, i.e. varying mechanical and anatomical properties of the cornea. The strong dependence of the force-indentation IOP calculation on the internal radius of curvature of the cornea as determined by a Keratonometer may introduce additional error.

References

1. Burns S and Miller D. Personal correspondence regarding through the eyelid tonometry. Fall 1999-Spring 2001.

2. Carlino R. *A Pressure Versus Displacement Measurement System.* MS Thesis MIT, 2000.

3. Fedorov SN et al. Method for estimation of intraocular pressure using free-falling ball. US Patent 5,176,139. 1993.

4. Fedorov SN et al. Ocular tonometer for estimation of intraocular pressure using free-falling ball. US Patent 5,197,473. 1993.

5. Fresco BB. A new tonometer - the pressure phosphene tonometer. *Ophthalmol* 1998; 105:2123-2126.

6. Fresco BB. Tonometer. US Patent 5,836,873. 1998.

7. Friedenwald JS. Contribution to the Theory and Practice of Tonometry. *Am J Opthalmol* Oct 1937;20:985-1012.

8. Friedenwald JS. Tonometer Calibration. *Trans Amer Acad of O & O* Jan-Feb 1957;108-122.

9. The Glaucoma Foundation. *Patient Guide.* http://www.glaucomafoundation.com/dihaq/index.htm. March 2001.

10. Greene PR. Closed-Form Ametropic Pressure-Volume and Ocular Rigidity Solutions. *Am J Ophthalmol* 1985;62:870-8.

11. Fung. *Biomechanics: Mechanical Properties of Living Tissues.* Berlin, Springer-Verlag. 1981.

12. Kaufman et al. *The Cornea.* Boston, Butterworth-Heinemann1998.

13. Mackie SW et al. Clinical comparison of the Keeler Pulsair 2000, American Optical MkII and Goldmann applanation tonomters. *Opthal Physiol Opt* 1996;16:171-7.

14. Ottensmeyer, MP. *Minimally Invasive Instrument for In Vivo Measurement of Solid Organ Mechanical Impedance.* Ph.D Thesis MIT, 2001.

15. Pierard GE et al. Ageing and rheological properties of facial skin in women. *Gerontology* 1998;44:159-61.

16. Schottenstein EM. *The Glaucomas: Basic Sciences* V.1, Second Edition, Chapter 20. Mosby-Year Book, Inc. 1996.

17. Stewart. *System of Ophthalmology: The Fundamentals of Ophthalmology*, Vol VI. St Louis, The CV Mosby Company, 1996.

18. Suzuki T. Tonometer. US Patent 5,349,955. 1994.

19. Takema Y et al. Age-related changes in the elastic properties and thickness of human facial skin. *Br J Dermatol* 1994;131:641-8.

20. van der Werff TJ. A new single-parameter ocular rigidity function. *Am J Ophthalmol* 1981;92:391-5.

21. Whitacre MM, Stein R. Sources of Error With Use of Goldmann-type Tonometers. *Sur Ophthalmol* 1993;38:1-34.

22. Woo SL et al. Analysis of the Corneo-Scleral Shell by the Method of Direct Stiffness. *J Biomechanics* 1971;4:323-30.

23. Woo SL et al. Mathematical Model of the Corneo-Scleral Shell as Applied to Intraocular Pressure-Volume Relations and Applanation Tonometry. *Ann Biomed Eng* 1972;1:87-98